

for nonpolar liquids. Explanations of vapor-liquid changes in terms of  $P_M$  may be directly tested by comparison with high-pressure experiments.

This viewpoint unifies the theoretical explanations of vapor, liquid, and high-pressure molecular properties. It also lends more general importance to high-pressure studies because molecules under high pressure are not in an unusual state. The high-pressure state is common to most chemical systems.<sup>77</sup>

(77) NOTE ADDED IN PROOF. It is recognized that eq 7-10 are very approximate. For example, the change in overlap in (10) might be better approximated by Roothaan's formulas (C. C. J. Roothaan, *J. Chem. Phys.*, **19**, 1445 (1951)); but, since the exact structures of a complex are unknown, it is thought that the simple calculations serve to illustrate the correct direction and approximate magnitude of CT spec-

**Acknowledgments.** The author thanks Dr. S. J. Strickler and Dr. J. N. Murrell for valuable discussions of electronic spectra. Dr. N. Snider has provided help on theories of liquids. This work was generously sponsored by Dr. M. W. Hanna and was done in his laboratory. The author has received partial support from the National Science Foundation.

tral changes. Since this article was submitted, a similar explanation of gas-liquid CT spectra has been received from J. Prochorow and A. Tramer, *J. Chem. Phys.*, **44**, 4545 (1966). The spectral results given by Prochorow and Tramer are in excellent agreement with the treatment here in terms of  $P_M$ . However, it is not necessary to postulate a quasi-crystalline solvent cage since high internal compression is obtained from the assumption of an unstructured liquid. Calculations correlating CT frequencies with  $P_M$  have been completed and will be published soon.

## Kinetics of Formation of N-Pyruvylidenglycinatozinc (II)<sup>1</sup>

D. L. Leussing and C. K. Stanfield

*Contribution from the Department of Chemistry, The Ohio State University, Columbus, Ohio 43210. Received July 25, 1966*

**Abstract:** N-Pyruvylidenglycinatozinc(II) is formed through two major pathways in the range pH 4.5-6.0. In one of these paths the rate-determining step appears to be the proton-catalyzed addition of glycinate to pyruvate followed by the splitting out of water from the carbinolamine. In the other path, zinc(II) ions appear to stabilize the carbinolamine through coordination. However, dehydration of this complex is effected through proton catalysis. In this system, the metal ions serve the role of stabilizing intermediates and products by forming complexes, but are much less effective than protons in influencing those reactions which are facilitated by a change of the charge distribution within the reactant molecules.

A series of investigations currently underway in our laboratories concerns the properties of the metal ion complexes of Schiff bases, particularly with their role in duplicating enzymatic reactions.<sup>2</sup> It was observed in our studies that the rates of formation of these complexes from the dissociated ligands lie in a range that is tractable for ordinary measurement. In order to fully understand the role of metal ions in catalyzing the reactions observed in nonenzymatic systems, it is necessary to have knowledge of the factors involved in their formation and dissociation. Furthermore, carbonyl addition reactions have been of interest to chemists for many years,<sup>3</sup> but relatively little is known regarding the kinetic effects of metal ions on these systems although their mediating effect on Schiff base formation is well recognized.<sup>4-6</sup> Thompson and Busch<sup>6</sup> have suggested that the metal ion in these systems can function as either a "kinetic template" or an "equilibrium template."

An earlier study by Nunez and Eichhorn<sup>7</sup> on the kinetics of formation of salicylidenglycinatonickel(II)

in dioxane-water mixtures suggested that metal ions slow the rate of formation of the Schiff base. Faster rates of formation were observed when the metal ion was added to a premixed solution of salicylaldehyde and sodium glycinate than when one of these ligands was added to a solution containing the metal ion and the other ligand. In these latter experiments, evidence for a two-step mechanism was found. It was postulated that the intermediate is a ternary (mixed) complex in which the ligands are independently bound, SMG ( $S^-$  = salicylaldehyde anion,  $G^-$  = glycinate anion). This mechanism would fall into the "kinetic template" category.

Salicylaldehyde and glycinate form a stable protonated Schiff base,  $SGH^-$ ,<sup>8,9</sup> similar to that formed in amino acid-pyridoxal<sup>10</sup> systems, and the faster rate of equilibration observed with the premixed ligands may merely indicate the fast proton displacement from already formed Schiff base.



Furthermore, no attempt was made to control the pH of the solutions in the earlier work<sup>7</sup> and the release of a proton when the Schiff base complex is formed obscures an interpretation of the reaction mechanism: carbonyl addition reactions show either proton or general acid catalysis,<sup>3</sup> and the released proton competes

(1) Paper VI in this series; paper V, D. L. Leussing and N. Hug, *Anal. Chem.*, **38**, 1388 (1966). This work was supported by the National Science Foundation, GP 1627. C. K. S. held an undergraduate research fellowship sponsored by The Ohio State University.

(2) D. E. Metzler, M. Ikawa, and E. E. Snell, *J. Am. Chem. Soc.*, **76**, 648 (1954).

(3) For recent discussions see, W. P. Jencks, *Progr. Phys. Org. Chem.*, **2**, 63 (1964); R. B. Martin, *J. Phys. Chem.*, **68**, 1369 (1964).

(4) H. Schiff, *Ann. Chem. Pharm.*, **150**, 193 (1869).

(5) P. Krumholz, *J. Am. Chem. Soc.*, **75**, 2163 (1953).

(6) M. C. Thompson and D. H. Busch, *ibid.*, **86**, 213 (1964).

(7) L. J. Nunez and G. L. Eichhorn, *ibid.*, **84**, 901 (1962).

(8) D. Heinert and A. E. Martell, *ibid.*, **85**, 183 (1963).

(9) K. Bai, unpublished results in these laboratories.

(10) D. E. Metzler, *J. Am. Chem. Soc.*, **79**, 485 (1957).

with the metal ion for glycinate thereby displacing the equilibrium position.

Earlier<sup>11</sup> it had been found in these laboratories that solutions of zinc(II), pyruvate ( $P^-$ ), and glycinate form the species  $ZnPG$ ,  $ZnPG_2^-$ , and  $ZnP_2G_2^{2-}$ . Proton magnetic resonance confirmed the presence of the azomethine linkage in these complexes.<sup>12</sup> In the present investigation the kinetics of formation of  $ZnPG$  were examined using a pH-Stat method. Spectrophotometric measurements were made to give an independent check of the rate constants obtained. The results provide further information regarding an important class of reactions.

### Experimental Section

A Radiometer pH-Stat equipped with an ABU-1 autoburet and a scale expander was used. Solutions containing known amounts of zinc chloride and pyruvic acid were freshly made up prior to each run. Most of the solutions also contained 0.50 M KCl, but in some experiments a medium of 0.10 M KCl was employed. An aliquot (usually 5.00 ml) was placed in a titration cell thermostated at 25°. The pH-Stat was set to the desired pH and the reaction was initiated. A standard sodium glycinate solution was introduced into the reaction medium from the autoburet. The volume of sodium glycinate added was recorded as a function of time.

The reaction proceeded in two distinct phases. The first phase consisted of the rapid neutralization of the pyruvic acid to give pyruvate ions and dipolar glycine molecule. It was necessary to have a known concentration of neutral glycine present so the pH values could be interpreted in terms of the concentration of free glycinate ions. The amount of glycine present was varied in some experiments by partially preneutralizing the pyruvic acid with standard NaOH. Simple pyruvate and glycinate complexes were also formed during this initial stage. The formation of these complexes may be considered complete in the few seconds required for the titrant to bring the solution to the predetermined value of pH.<sup>13</sup>

The second phase of the reaction was observable after the reaction pH was attained by the solution. A slower rate of sodium glycinate addition signified the formation of the Schiff base complex. As the glycinate concentration decreased through the formation of  $ZnPG$ , the pH of the solution decreased. Additional reagent was added from the autoburet to restore the pH to the desired value. The solution pH fluctuated by about  $\pm 0.01$  pH unit around a mean value. The reaction was followed to completion and the equilibrium pH of the solution was accurately determined.

Rate data were obtained in the pH range 4.5–6.0. Below this lower limit the free energy of reaction is unfavorable and the extent of complex formation is too slight to give accurate rate data. This was found to be the situation even at pH 4.5 when low Zn(II) levels were employed. The upper pH limit arises from the extensive initial formation of zinc(II)-glycinate complexes which serve as a reservoir for glycinate. The imine complex forms using glycinate furnished by the decomposition of the simple complexes rather than requiring an external source. This observation does not imply a particular reaction mechanism since the same effect would be observed whether pyruvate reacted directly with a glycinatezinc complex or the zinc complex first dissociated and the liberated glycinate reacted *via* another path. Even at pH 6.0 the decrease in sensitivity of the measured rate of addition to the actual reaction rate produced more scatter in the data than was observed at lower pH values.

The total glycinate level was varied from 0.04 to 0.10 M, total zinc was varied from 0.0085 to 0.13 M, and the range of total pyruvate was 0.009 to 0.060 M. Complex formation together with pH variation yielded the following concentration ranges for the free species:  $Zn^{2+}$ , 0.0035 to 0.096 M;  $P^-$ , 0.0079 to 0.042 M;  $G^-$ ,  $2.5 \times 10^{-7}$  to  $8.35 \times 10^{-6}$  M.

### Calculations

The reaction rate was calculated from the slope,  $dv/dt$ , of the volume-time curve at the onset of the

(11) D. L. Leussing, and D. C. Schulz, *J. Am. Chem. Soc.*, **86**, 4846 (1964).

(12) D. L. Leussing and C. K. Stanfield, *ibid.*, **86**, 2806 (1964).

(13) M. Eigen and R. G. Wilkins, "Mechanisms of Inorganic Reactions," *Advances in Chemistry Series*, No. 49, American Chemical Society, Washington, D. C., 1965, p 55.

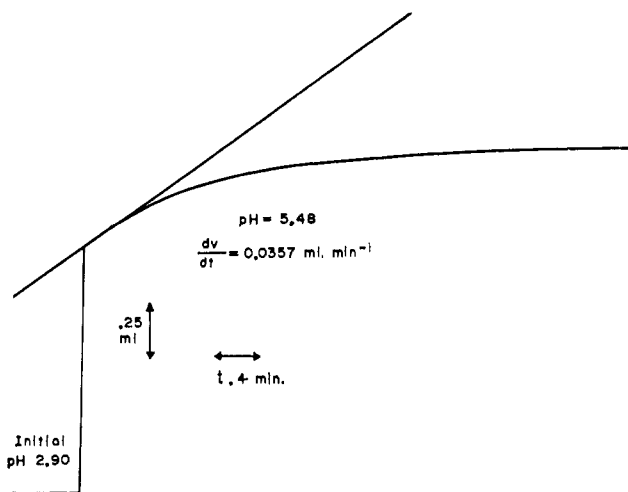


Figure 1. Experimental volume-time curve:  $(G^-)_{tot} = 0.0509 M$ ,  $(Zn)_{tot} = 0.04894 M$ ,  $(P^-)_{tot} = 0.01625 M$ ,  $(H^+)_{tot} = 0.0411 M$ ,  $Zn^{2+} = 0.0356 M$ ,  $P^- = 0.0095 M$ ,  $G^- = 2.49 \times 10^{-6} M$ .

second phase ( $t = 0$ ). An example of an experimental volume-time curve and the calculation of  $dv/dt$  is shown in Figure 1.

In order to obtain the rate of formation of  $ZnPG$ ,  $d(ZnPG)/dt$ , and to determine the kinetic rate law, it is necessary to know the concentrations of all the species which are present at the onset of the second phase.

Mass balance of the known total concentrations and application of equilibrium relationships allow the following equations to be written

$$(Zn)_{tot} = (Zn^{2+})[1 + \beta_{01}(G^-) + \beta_{02}(G^-)^2 + \beta_{03}(G^-)^3 + \beta_{10}(P^-) + \beta_{20}(P^-)^2] + (ZnPG)$$

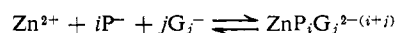
$$(P^-)_{tot} = \left[ \frac{(H^+)}{K_{ap}} + 1 \right] (P^-) + \beta_{10}(Zn^{2+})(P^-) + 2\beta_{20}(Zn^{2+})(P^-)^2 + (ZnPG)$$

$$(H^+)_{tot} = (H^+) - (OH^-) + \frac{(H^+)(P^-)}{K_{ap}} + \left[ \frac{2(H^+)^2}{K_{1aG}K_{2aG}} + \frac{(H^+)}{K_{2aG}} \right] (G^-)$$

$$(G^-)_{tot} = \left[ \frac{(H^+)^2}{K_{1aG}K_{2aG}} + \frac{(H^+)}{K_{2aG}} + 1 \right] (G^-) + \beta_{01}(Zn^{2+})(G^-) + 2\beta_{02}(Zn^{2+})(G^-)^2 + 3\beta_{03}(Zn^{2+})(G^-)^3 + (ZnPG)$$

$$(ZnPG)_{t=0} = 0; \quad \beta_{ij} = \frac{(ZnP_iG_j)}{(Zn^{2+})(P^-)^i(G^-)^j}$$

for the reaction



$$\beta_{01} = 7.6 \times 10^4 \quad \beta_{02} = 1.02 \times 10^9 \quad \beta_{03} = 1 \times 10^{11}$$

$$\beta_{10} = 18.1 \quad \beta_{20} = 96.3$$

$$K_{ap} = 4.1 \times 10^{-3}$$

$$K_{1aG} = 3.5 \times 10^{-3} \quad K_{aG} = 2.0 \times 10^{-10}$$

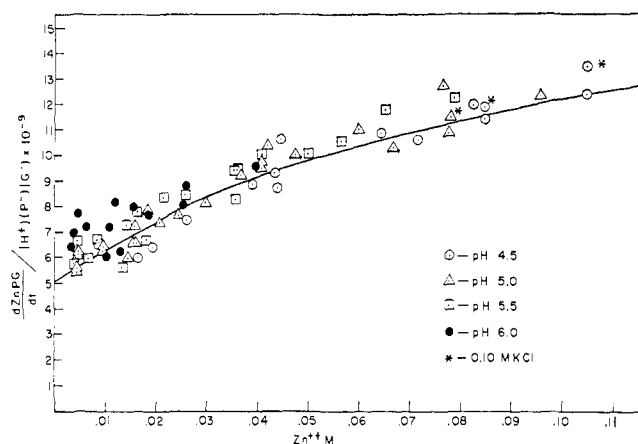


Figure 2. Rate of ZnPG formation as a function of free  $Zn^{2+}$  concentration.

The pH is known at each point so only the first three of these equations are required to calculate the equilibrium values of  $Zn^{2+}$ ,  $P^-$ , and  $G^-$ . Solutions were obtained using the Newton-Raphson method.

A check on the consistency of each reaction system was made by using the fourth equation to calculate a value of  $(G^-)_{tot}$ , which then was compared with the observed value. Considering the uncertainties in calculating exact equilibrium concentrations, the agreement between observed and calculated values of  $(G^-)_{tot}$  was good for most points ( $\sigma_r = 2$  to 5%). A tendency for the observed values to be greater than those calculated may have arisen partially from a lag in the pH-Stat. The autoburet tended to overshoot and not stop the infusion of titrant exactly when the nominal pH had been reached at the end of the first phase. Attempts to interpret the high values in terms of the rapid formation of ZnPG in a form where the ligands are independently bound was not successful: widely varying values of the apparent formation of this postulated species resulted.

Owing to the formation of the simple glycinatozinc(II) complexes and their function as a source of glycinate, values of  $d(ZnPG)/dt$  cannot be obtained directly from the observed values of  $dv/dt$  except in the low pH range. The four mass balance equations written above must be differentiated to give

$$\begin{aligned} \frac{d(Zn)_{tot}}{dt} &= [1 + \beta_{01}(G^-) + \beta_{02}(G^-)^2 + \beta_{03}(G^-)^3 + \\ &\quad \beta_{10}(P^-) + \beta_{20}(P^-)^2] \frac{d(Zn^{2+})}{dt} + \\ &\quad (Zn^{2+})[\beta_{01} + 2\beta_{02}(G^-) + 3\beta_{03}(G^-)^2] \frac{d(G^-)}{dt} + \\ &\quad (Zn^{2+})[\beta_{10} + 2\beta_{20}(P^-)] \frac{d(P^-)}{dt} + \frac{d(ZnPG)}{dt} \\ \frac{d(P)_{tot}}{dt} &= \left[ \frac{(H^+)}{K_{ap}} + 1 \right] \frac{d(P^-)}{dt} + [\beta_{10}(P^-) + \\ &\quad 2\beta_{20}(P^-)^2] \frac{d(Zn^{2+})}{dt} + (Zn^{2+})[\beta_{10} + 4\beta_{20}(P^-)] \frac{d(P^-)}{dt} + \\ &\quad \frac{d(ZnPG)}{dt} \end{aligned}$$

$$\begin{aligned} \frac{d(H)_{tot}}{dt} &= \frac{(H^+)}{K_{ap}} \frac{d(P^-)}{dt} + \left[ \frac{2(H^+)^2}{K_{1aG}K_{2aG}} + \frac{(H^+)}{K_{2aG}} \right] \frac{d(G^-)}{dt} \\ \frac{d(G)_{tot}}{dt} &= \left[ \frac{(H^+)^2}{K_{1aG}K_{2aG}} + \frac{(H^+)}{K_{2aG}} + 1 \right] \frac{d(G^-)}{dt} + \\ &\quad [\beta_{01}(G^-) + 2\beta_{02}(G^-)^2 + 3\beta_{03}(G^-)^3] \frac{d(Zn^{2+})}{dt} + \\ &\quad (Zn^{2+})[\beta_{01} + 4\beta_{02}(G^-) + 9\beta_{03}(G^-)^2] \frac{d(G^-)}{dt} + \\ &\quad \frac{d(ZnPG)}{dt} \end{aligned}$$

These four equations are linear in the four unknowns  $d(Zn^{2+})/dt$ ,  $d(P^-)/dt$ ,  $d(G^-)/dt$ , and  $d(ZnPG)/dt$ . The values of  $d(Zn)_{tot}/dt$ ,  $d(P)_{tot}/dt$ , and  $d(H)_{tot}/dt$  are small and arise from the dilution of the solution by the titrant. The value of  $d(G^-)_{tot}/dt$  is related to  $dv/dt$  by

$$\frac{d(G^-)_{tot}}{dt} = \frac{C_G - (G^-)_{tot} dv}{V dt}$$

$C_G$  is the concentration of sodium glycinate in the titrant, and  $V$  is the total volume of the solution (the initial volume plus titrant added in the first phase).

Solving simultaneously using the values of  $Zn^{2+}$ ,  $P^-$ ,  $G^-$ , and  $H^+$  calculated previously yields the values of the derivatives.

## Results

Inspection of the data indicated that within the scatter of the points, the rate of formation of ZnPG is first order in each of  $(H^+)$ ,  $(P^-)$ , and  $(G^-)$ . The quantity  $[d(ZnPG)/dt]/[(H^+)(P^-)(G^-)]$  plotted vs.  $(Zn^{2+})$  caused all the points with the possible exception of those at pH 6.0 to fall along one curve. This plot is shown in Figure 2. The scatter primarily arises from the uncertainties in evaluating  $(Zn^{2+})$ ,  $(G^-)$ , and  $(P^-)$  and the carry-over of these uncertainties into the values computed for  $d(ZnPG)/dt$ .

In Figure 2 it is seen that the points extrapolate to a finite value on the ordinate. This indicates that a major path exists which is independent of  $(Zn^{2+})$ . The zinc ions, while not kinetically active along this path, trap the reaction product to provide a favorable free energy. The increase in the rate with increasing  $(Zn^{2+})$  shows that a parallel Zn(II) active path also exists. The downward curvature toward an upper limiting rate indicates that this second path involves more than one step and at high  $(Zn^{2+})$  levels, a  $(Zn^{2+})$  independent step becomes rate-determining.

A reaction sequence which is consistent with these observations and which also incorporates the essential features proposed for Schiff base formation in the absence of metal ions<sup>3</sup> is

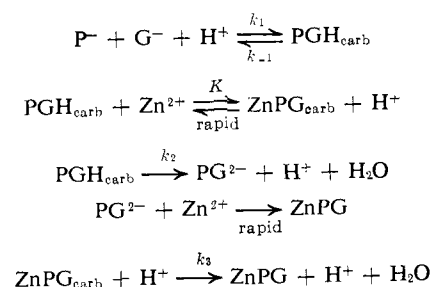


Table I. A Comparison of Pseudo-First-Order Rate Constants for Pyruvate Disappearance

Total Zn(II), M	Total NaG, M	(GH), M	(Zn <sup>2+</sup> ), M	(G <sup>-</sup> ) × 10 <sup>6</sup> , M	pH	k' <sub>spec</sub>	k' <sub>pH</sub>
0.0475	0.0099	0.10	0.038	3.5	5.28	0.0026	0.0028
0.0475	0.0099	0.07	0.038	3.5	5.46	0.0022	0.0018
0.0380	0.0148	0.05	0.023	8.4	6.08	0.0019	0.0009

The species subscripted by carb represent the carbinolamine form<sup>3</sup> of the pyruvate-glycinate addition product.

Applying the steady-state approximation to the carbinolamine intermediates yields the rate expression

$$\frac{d(\text{ZnPG})}{dt} = k_1 \left[ \frac{\frac{k_2}{k_3K} + (\text{Zn}^{2+})}{k_{-1} + k_2 + \frac{k_2}{k_3K} + (\text{Zn}^{2+})} \right] (\text{H}^+)(\text{P}^-)(\text{G}^-)$$

Fitting the points in Figure 2 (except those at pH 6.0) to this expression yields the least-squares values

$$k_1 = 3.3 \times 10^8 \text{ mole}^{-2} \text{ l.}^{-2} \text{ sec}^{-1}$$

$$k_2/k_3K = 0.0275 \text{ mole l.}^{-1}$$

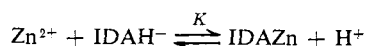
$$(k_{-1} + k_2)/k_3K = 0.106 \text{ mole l.}^{-1}$$

The solid line in Figure 2 represents the theoretical curve calculated using these results.

Equilibrium data reported in the literature yield supporting evidence that, in the pH and (Zn<sup>2+</sup>) range employed here, conversion of the intermediate carbinolamine from the protonated form, PGH<sub>carb</sub>, to the complex, ZnPG<sub>carb</sub>, may occur. Iminodiacetate, <sup>-</sup>O<sub>2</sub>C-CH<sub>2</sub>NHCH<sub>2</sub>CO<sub>2</sub><sup>-</sup>, is analogous to the proposed intermediate, <sup>-</sup>O<sub>2</sub>CCH<sub>2</sub>NHCH(OH)(CH<sub>3</sub>)CO<sub>2</sub><sup>-</sup> (= PG<sub>carb</sub><sup>2-</sup>). For IDA<sup>2-</sup>



The reaction constant for the exchange of a proton by Zn<sup>2+</sup>



is calculated from these values to be  $8 \times 10^{-3}$ . The log of the ratio (IDAZn<sup>+</sup>)/(IDA<sup>H-</sup>) for various values of Zn<sup>2+</sup> and pH is presented in Figure 3, where it is seen that under the range of pH values and Zn<sup>2+</sup> concentrations employed, this ratio lies within about an order of magnitude, and on both sides, of unity.

The effect of -OH and Me substitution will certainly cause the pK<sub>a</sub> value of the carbinolamine to differ from that of IDA<sup>2-</sup>, but since only σ bonding is involved, it is expected that the formation constant of ZnPG<sub>carb</sub> will differ by a similar factor from that of IDAZn. Thus, the exchange constant, K, likely will not differ greatly from IDA<sup>2-</sup> to PG<sub>carb</sub><sup>2-</sup>. A distribution similar to that presented in Figure 3 should prevail in the pyruvate-glycinate system.

(14) S. Chaberek and A. E. Martell, *J. Am. Chem. Soc.*, **74**, 5052 (1952).

If the concentration of the intermediate carbinolamine is very low, those metal ion steps which have been postulated to be rapid will also add to the rate-determining processes. The present data, however, are not sufficiently precise to cast light on this point.

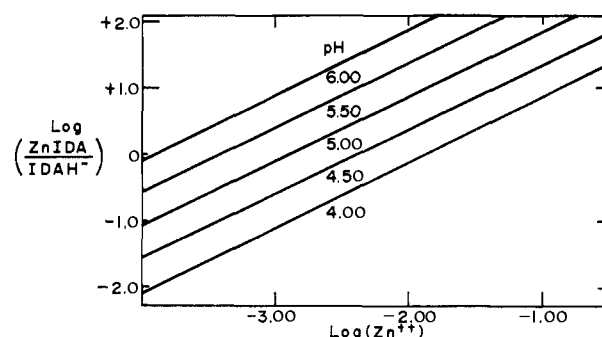


Figure 3. Ratio of complexed to protonated form of a model ligand under the conditions described in Table I. IDA<sup>2-</sup> = iminodiacetate.

It is significant that the dehydration of ZnPG<sub>carb</sub> requires proton catalysis. This suggests that, in the pH range investigated here at least, the metal ion is much less effective in inducing electron rearrangements within the organic moiety than is the proton.

**Spectrophotometric Determination of Rate of Pyruvate Reaction.** Pyruvate ion shows an absorption maximum at 315 mμ (ε 25). The absorption of the Schiff base at this wavelength is much less intense so it is possible to directly determine the rate of disappearance of pyruvate in solutions of zinc glycinate. Pyruvate was added to a premixed solution containing an excess of zinc(II) and glycinate ions. The absorbance of the solution in 10.0-cm cells was monitored at 315 mμ. The pseudo-first-order rate constant for the disappearance of pyruvate was calculated from the absorbance changes

$$-d(\text{P}^-)/dt = k'_{\text{spec}}(\text{P}^-)$$

According to the mechanism postulated from the pH-Stat measurements

$$\frac{d(\text{ZnPG})}{dt} = -\frac{d(\text{P}^-)}{dt} = k'_{\text{pH}}(\text{P}^-)$$

where

$$k'_{\text{pH}} = k_1 \left[ \frac{k_2 k / k_3 K + (\text{Zn}^{2+})}{[(k_{-1} + k_2) / k_3 K + (\text{Zn}^{2+})](\text{H}^+)(\text{G}^-)} \right]$$

The results given in Table I show that satisfactory agreement is obtained between the observed values

